

Patterns of tropospheric response to solar variability

Hans Gleisner and Peter Thejll

Climate and Solar-Terrestrial Physics Divisions, Danish Meteorological Institute, Copenhagen, Denmark

Received 14 February 2003; revised 16 May 2003; accepted 28 May 2003; published 12 July 2003.

[1] Despite numerous reports of apparent climate responses to the 11-year solar cycle, the Sun's role for weather and climate has remained a matter of controversy. One important reason is the difficulty of reliably attributing the observed atmospheric effects to solar variability, rather than to other forcing factors or intrinsic variability. Here we show that consistent patterns of statistically significant solar signals emerge in all major observables throughout the low- and mid-latitude troposphere, when El Niño and volcanic signals are removed from meteorological data. Solar forcing is strongest in the tropics and at mid-latitudes, and the heating and moistening of the troposphere during solar maximum is accompanied by a modulation of the large-scale tropospheric circulation systems. These findings have implications for the question of where and how the Sun exerts its influences in the climate system. **INDEX TERMS:** 1650 Global Change: Solar variability; 3309 Meteorology and Atmospheric Dynamics: Climatology (1620); 3319 Meteorology and Atmospheric Dynamics: General circulation. **Citation:** Gleisner, H., and P. Thejll, Patterns of tropospheric response to solar variability, *Geophys. Res. Lett.*, 30(13), 1711, doi:10.1029/2003GL017129, 2003.

1. Introduction

[2] Apparent climate responses to the 11-year solar cycle have been reported in the scientific literature for more than a century [e.g., Hoyt and Schatten, 1997]. Observational findings suggest solar-cycle variations of the stratospheric thermal and geopotential structure [van Loon and Labitzke, 1993; van Loon and Shea, 2000], globally averaged lower-tropospheric temperatures [Douglass and Clader, 2002], sea-surface temperatures [White et al., 1997], sea-level pressures [Kelly, 1977], and the global amount of low clouds [Svensmark and Friis-Christensen, 1997; Marsh and Svensmark, 2000]. Despite these and numerous other reports, the Sun's role for weather and climate has remained a matter of controversy. The reasons for this state of affairs may be the confusing disparity of the findings and the lack of established physical mechanisms that could amplify an energetically weak solar signal. An equally important reason is the difficulty of reliably attributing the observed atmospheric effects to solar variability, rather than to other forcing factors acting on similar time-scales. Both the ENSO phenomenon and stratospheric aerosols of volcanic origin influence the tropospheric climate, globally and on an inter-annual timescale [Michaels and Knappenberg, 2000].

[3] Here we perform a study of inter-annual to decadal solar signals in the troposphere, utilizing a 3-D gridded

meteorological data set from which El Niño and volcanic effects are removed together with the effects of any forcing factors that primarily are expressed as trends in the climate data, e.g., tropospheric aerosols or greenhouse gases. This correction of the data results in an increased clarity of the solar signals, and allows us to rule out the two most important competing forcing factors as a cause of the apparent solar effects. We show that significant solar signals are found in all major observables throughout the low- and mid-latitude troposphere, and that a spatially heterogeneous response pattern emerges in which water vapor and the large-scale tropospheric circulation systems play important roles. These findings have implications for the question of where and how solar variability affects the climate system.

2. Data and Methods

[4] This study is based on the NCEP/NCAR reanalysis data set [Kalnay et al., 1996]. The term "reanalysis" refers to the generation of physically consistent, 3-D gridded meteorological data through the assimilation of observational data into a physical model. Some of the data (temperature, geopotential height, horizontal velocity) are primarily governed by observations, while other data (humidity, vertical velocity) are influenced by the model itself to a higher degree. Due to the sparsity of observations, humidity is more model dependent than temperatures or geopotential heights. Throughout this study, solar forcing is quantified by the solar 10.7 cm radio flux $F_{10.7}$. In the absence of knowledge about physical mechanisms, and considering its strong correlations to other solar-activity parameters, $F_{10.7}$ can be regarded as a general proxy for the as yet unknown solar forcing factor, or factors, varying in concert with the 11-year solar cycle.

[5] Annual means are computed from monthly anomaly data which have been corrected for El Niño and volcanic effects using a multi-variate regression procedure. Each atmospheric observable is described by

$$O = k_0 + k_1 \text{NINO3} + k_2 F_{10.7} + k_3 \text{AOD} + k_4 F_{lin} + \varepsilon$$

where NINO3 is the mean sea-surface temperature in the equatorial Pacific (5°N–5°S, 150°W–90°W), AOD is the global stratospheric Aerosol Optical Depth [Sato et al., 1993], and F_{lin} is a linear trend. The coefficients k_n are obtained independently for each spatial location through multi-variate regression on monthly anomaly data. A time lag of 3 months is applied to NINO3 (see section 16.3 of [Peixoto and Oort, 1992]). No delays are applied to AOD or $F_{10.7}$. By subtracting the terms $k_1 \text{NINO3}$, $k_3 \text{AOD}$, and $k_4 F_{lin}$ from the observed data, O , we obtain the corrected data, O^* , which describe all atmospheric variations that are

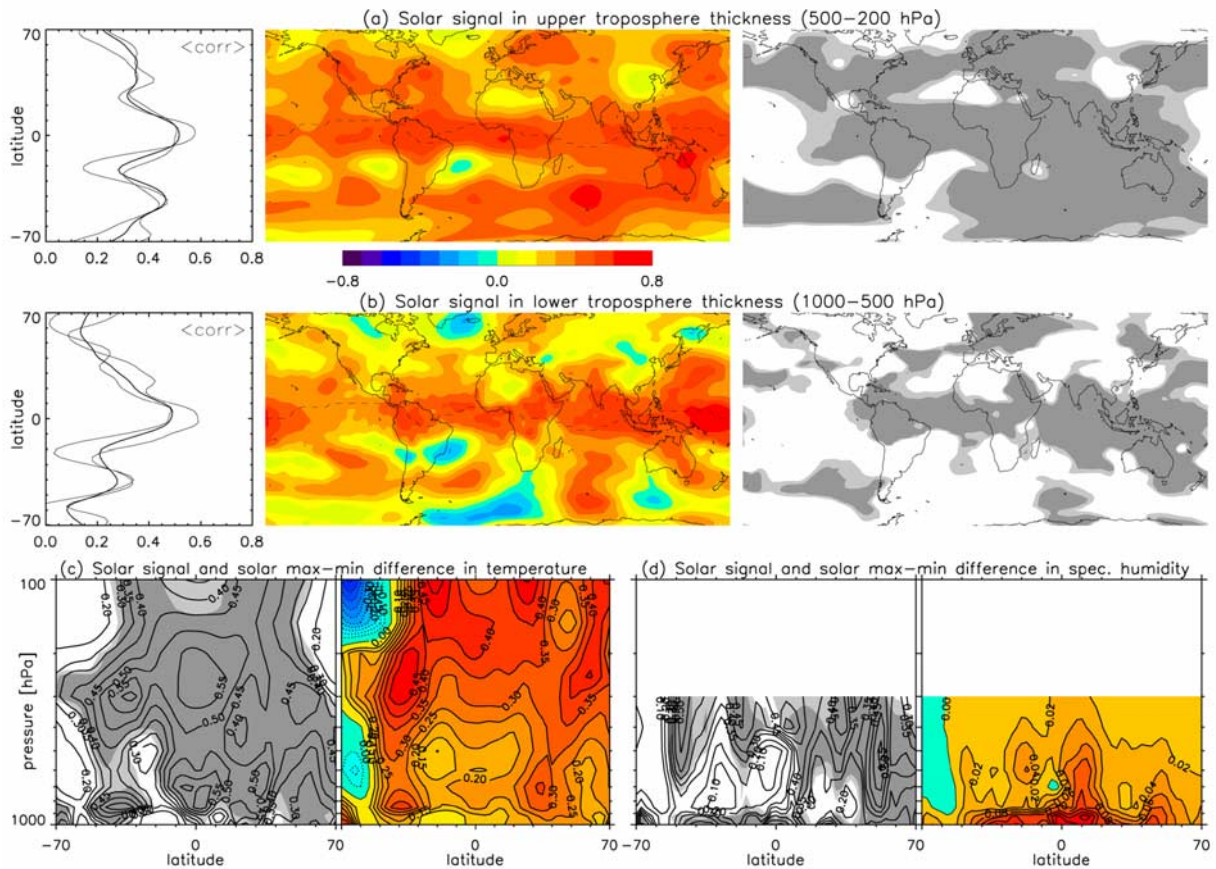


Figure 1. Solar signals in the troposphere: correlations between $F10.7$ and (a) upper tropospheric and (b) lower tropospheric thicknesses. The corresponding 90% and 95% significance levels are shown to the right, and zonal averages of the correlation coefficients are shown to the left; globally and in the two sectors $60^{\circ}\text{W}–10^{\circ}\text{E}$ and $140^{\circ}\text{E}–210^{\circ}\text{E}$. The panels at the bottom show correlations between $F10.7$ and (c) zonally averaged temperature T_{zon}^{\star} , and (d) zonally averaged specific humidity q_{zon}^{\star} . Grey shadings denote the 90% and 95% significance levels. The color plots (c–d) show the mean differences ΔT_{zon}^{\star} and Δq_{zon}^{\star} between solar cycle maximum (annual $F10.7 > 150$) and minimum (annual $F10.7 < 80$).

not explained by El Niño, stratospheric aerosols, or other forcing factors primarily expressed as trends in the climate data. It is assumed that any effects of removing spurious signals that are only incidentally correlated to the regression variables are small.

[6] Collinearity amongst regression variables can lead to uncertain regression coefficients while the overall fit still may be good. We test for such problems using singular value decomposition [Belsley, 1991]. Values of the conditioning index (the ratio between the largest and smallest singular values) near 30 indicate potential problems. In the present study this index never becomes larger than about 9, and collinearity is not likely to be a problem.

[7] The local significance levels are estimated from surrogate data with similar statistical properties as the original data, effectively addressing the problem of chance correlations with atmospheric variations of non-solar origin. The distribution of correlation coefficients is generated under the null hypothesis of no physical relationships, and from the top and bottom percentiles of this distribution we obtain the probability that a correlation as good as or better than the one observed would occur by chance. The surrogate data are generated by randomly scrambling the harmonic phases of the observed time

series [Theiler and Prichard, 1996], thus preserving the spectral power distribution.

3. Solar Signals in the Troposphere

[8] Throughout this study the solar signals in the troposphere are quantified by the local correlations between annual means of $F10.7$ and corrected atmospheric parameters, denoted by superscript \star . All correlations are based on data from 1958 to 2001, thus covering 4 solar cycles.

[9] The strongest solar signals are found in the geopotential structure. We have studied the thickness ΔZ^{\star} - defined as the height difference between two isobaric surfaces - of two tropospheric layers; an upper layer (500 to 200 hPa) and a lower layer (1000 to 500 hPa). Figures 1a–1b show correlations between $F10.7$ and ΔZ^{\star} for the two layers, along with the 90% and 95% significance levels. We first note that positive correlations predominate throughout the studied region, and that the solar signals show a pronounced three-banded structure. Two bands of high and significant correlations around latitudes $40^{\circ}–50^{\circ}$ are separated from an equatorial band of high correlations by minima around latitudes $20^{\circ}–30^{\circ}$. The equatorial band is almost equally strong in the two layers, while the mid-latitude bands are

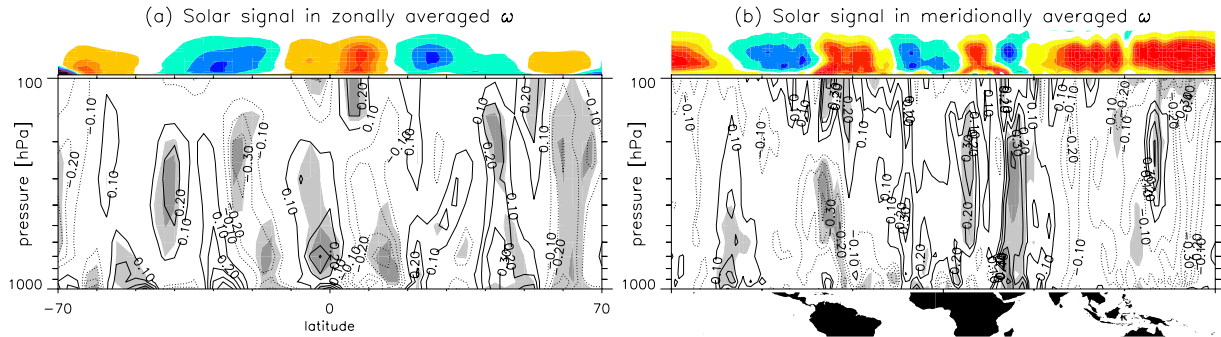


Figure 2. Solar signals in vertical motions: correlations between $F10.7$ and (a) zonally averaged vertical velocities ω^* , and (b) meridionally averaged, equatorial (12.5°S to 12.5°N) vertical velocities ω^* . Grey shadings denote the 80% and 95% significance levels. The climatology of ω is qualitatively outlined at the top of the panels, to indicate regions of upward (shades of yellow and red) and downward (blue and green) atmospheric motions. Note that ω is positive downwards.

considerably stronger in the upper layer. In the upper-tropospheric equatorial band (Figure 1a) we find the strongest solar signals, with correlations around 0.60, in the Atlantic sector, from the Amazon area to equatorial Africa, and in the western Pacific and the Indonesian archipelago. The mid-latitude bands (Figure 1a) show a considerable north-south asymmetry, the southern band being stronger and having a more regular appearance than the northern band. The strongest solar signals within the mid-latitude bands appear to be associated with the mean location of the polar fronts [Rumney, 1968], which are regions of high cyclonic activity. The pattern of solar signals in ΔZ^* shows a striking resemblance to the distribution of precipitation rates [Peixoto and Oort, 1992], which is known to be governed by tropical convection near the equator and by cyclonic disturbances along the polar fronts at mid-latitudes.

[10] Figure 1c (left panel) shows correlations between $F10.7$ and the zonally averaged temperature T_{zon}^* , together with the 90% and 95% significance levels. At the 300 hPa level there are three local maxima in the correlations, corresponding to the three bands. Closer to the tropopause, the equatorial band vanishes while two mid-latitude bands continue up into the stratosphere. The T_{zon}^* correlations reach peaks of around 0.60. Figure 1c (right panel) also shows a map of the mean difference ΔT_{zon}^* between solar cycle maximum (annual $F10.7 > 150$) and minimum (annual $F10.7 < 80$). A ΔT_{zon}^* of about 0.45 K is reached around 250 hPa at mid-latitudes.

[11] Figure 1d shows correlations between $F10.7$ and the zonally averaged specific humidity, q_{zon}^* , together with the 90% and 95% significance levels. The correlations are predominantly positive; higher solar activity is associated with more water vapor in the troposphere. The solar signals are strongest and most significant at 50° latitude in both hemispheres, reaching a correlation of about 0.55. Closer to the equator, the pattern of correlations appears to be asymmetric, being displaced toward the northern hemisphere. An association between solar signals in specific humidity and vertical motions can be discerned (compare Figures 1d and 2a).

[12] Another observation is the significant solar signal, and the high solar max-min difference Δq_{zon}^* , in the very lowest atmospheric layers. A plot of the $F10.7$ - q_{zon}^* correlations at the 1000 hPa level (not shown here) shows this

largely to be associated with oceanic regions in the tropics and at mid-latitudes. The two equatorial regions of peak solar signals in tropospheric layer thickness coincide with significant solar signals in near-surface humidity.

[13] We expect the heterogeneous response of temperatures, geopotential structure, and humidity to be accompanied by variations of atmospheric motions. Can solar signals be found directly in the velocities? Velocities have a high degree of spatial structure. The fact that they are vectorial quantities, and that solar signals tend to occur with opposite signs in neighboring regions, gives rise to a spatially complex picture in which solar signals are lost during spatial and temporal averaging. Figure 2 shows correlations between $F10.7$ and (a) zonally averaged vertical velocity ω^* , and (b) meridionally averaged (12.5°S to 12.5°N), equatorial ω^* . Note that ω is positive downwards. In the meridional average (Figure 2b) we find solar signals in regions of subsiding atmospheric motions, strongest in the equatorial eastern Africa, and in regions of ascending motions, most pronounced in the Amazon region. The solar signals in the east African region of subsiding motions can also be seen in the zonal plot (Figure 2a) as a weakening of the ascending motions that predominate near the equator.

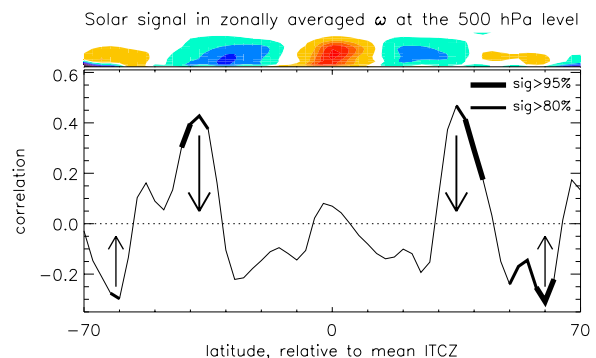


Figure 3. Correlations between $F10.7$ and zonally (relative to the mean ITCZ) averaged ω^* at the 500 hPa level. Note that ω is positive downwards. The arrows show the effects on ω by increased solar activity, indicating a strengthening of the Ferrel circulation. The vertical atmospheric motions are indicated at the top of the panel as in Figure 2.

This demonstrates a problem with zonal plotting of a variable that has substantial zonal asymmetries. By zonal averaging with respect to a mean Inter-Tropical Convergence Zone (ITCZ - dashed line in Figure 1), rather than the equator, we can partially correct for this. A result of this type of plotting can be seen in Figure 3 which shows solar signals in zonally averaged ω^* at the 500 hPa level. The solar signals now appear symmetric. Higher solar activity is associated with stronger subsidence at mid-latitudes, a poleward motion of the peak subsidence, and stronger ascending motions in the rising branch of the Ferrel circulation. When averaged along the ITCZ, there are no significant solar signals in the ascending branch of the Hadley circulation. There is, however, a tendency for higher solar activity to be associated with stronger ascending motions at the edge of the rising branch, leading to a latitudinal broadening of the upflow region. As shown in Figure 2b, there are also indications of a solar modulation of the Walker-type circulation parallel to the equator.

4. Discussion

[14] We here provide strong evidence for a significant response of the troposphere to the 11-year solar cycle, and show that the apparent solar signals are not merely due to chance covariations with El Niño or major volcanic eruptions. A tropospheric response pattern emerges showing how the low- and mid-latitude troposphere becomes warmer and moister during solar maximum. The response is spatially heterogeneous, being strongest in three latitudinal bands with local maxima in regions of deep tropical convection and of mid-latitude cyclonic activity.

[15] The solar signals in the velocity data are weaker than in the thermodynamic variables. However, the solar signals that do occur provide supporting evidence for a variation of the large-scale tropospheric circulation. Most notably, the solar signals in vertical velocity indicate a modulation of the Ferrel circulation together with a spatially heterogeneous modulation of the Hadley and Walker-type circulations.

[16] Our findings appear to be related to those reported in, e.g., Labitzke and van Loon [1995]. Without removing volcanic or El Niño signals, they show that the solar cycle correlates with stratospheric geopotential heights and tropospheric temperatures. The decrease in low-latitude vertical temperature gradients from solar minimum to maximum, a consequence of the temperature structure shown in Figure 1c which indicates enhanced latent heat release in the upper tropical troposphere, have lead Labitzke and van Loon to the conclusion that the tropical convection undergoes a solar-cycle modulation. We here find strong support for the wider notion of an atmospheric response that involves the global-scale tropospheric circulation systems.

[17] The findings presented here may have implications for the question of where and how the Sun exerts its influences in the climate system. Global circulation models have been used to estimate the atmospheric effects of a variable solar total or UV irradiance [e.g., Haigh, 1999; Shindell et al., 1999; Meehl et al., 2003]. The tropospheric response patterns presented here might help discriminate between these two type of solar-irradiance forcing mechanisms. They may also help improve our understanding of the

role played by the apparent solar-cycle variation of low clouds [Marsh and Svensmark, 2000], a potentially important source of radiative forcing of the climate. A fundamental question - perhaps central to the Sun-climate field - is how the clouds are modulated. Svensmark and Friis-Christensen [1997] have suggested that low clouds are modulated by cosmic rays, whereas others [Kristjánsson et al., 2002] regard solar radiation as a more likely cause of the observed effects. We have here shown how the troposphere responds to solar activity. A key question is then how the clouds in turn respond to these changes. With an improved quantitative understanding of cloud-climate relationships, we may be able to discriminate between the two hypotheses.

[18] **Acknowledgments.** Most of the data were obtained from various NOAA web sites: the reanalysis data from the CDC web site, the NINO 3 index from the CPC web site, and the solar $F_{10.7}$ index from the NGDC web site. The AOD data were obtained from NASA's GISS web site. This work was supported by the Danish Climate Centre, and by an ESA Research Fellowship.

References

- Belsley, D. A., *Conditioning Diagnostics - Collinearity and Weak Data in Regression*, John Wiley, New York, 1991.
- Douglass, D. H., and B. D. Clader, Climate sensitivity of the Earth to solar irradiance, *Geophys. Res. Lett.*, doi:10.129/2002GL015345, 2002.
- Haigh, J. D., Modelling the impact of solar variability on climate, *J. Atmos. Terr. Phys.*, 61, 63–72, 1999.
- Hoyt, D. V., and K. H. Schatten, *The role of the sun in Climate change*, Oxford University Press, New York, 1997.
- Kalnay, E., et al., The NCEP/NCAR 40-Year Reanalysis Project, *Bull. Am. Met. Soc.*, 77, 437–531, 1996.
- Kelly, P. M., Solar influence on North Atlantic mean sea level pressure, *Nature*, 269, 320–322, 1977.
- Kristjánsson, J. E., A. Staple, J. Kristiansen, and E. Kaas, A new look at possible connections between solar activity, clouds and climate, *Geophys. Res. Lett.*, doi:10.129/2002GL015646, 2002.
- Labitzke, K., and H. van Loon, Connection between the troposphere and the stratosphere on a decadal scale, *Tellus A*, 47, 275–286, 1995.
- Marsh, N., and H. Svensmark, Low cloud properties influenced by cosmic rays, *Phys. Rev. Lett.*, 85, 5004–5007, 2000.
- Meehl, G. A., et al., Solar and greenhouse gas forcing and climate response in the 20th century, *J. Clim.*, 16, 426–444, 2003.
- Michaels, P. J., and P. C. Knappenberg, Natural signals in the MSU lower tropospheric temperature record, *Geophys. Res. Lett.*, 27, 2905–2908, 2000.
- Peixoto, J. P., and A. H. Oort, *Physics of Climate*, Springer Verlag, New York, 1992.
- Rumney, G. R., *Climatology and the World's Climate*, p. 67, MacMillan, New York, 1968.
- Sato, M., J. E. Hansen, M. P. McCormick, and J. B. Pollack, Stratospheric aerosol optical depth 1850–1990, *J. Geophys. Res.*, 98, 22,987–22,994, 1993.
- Shindell, D., D. Rind, N. Balachandran, J. Lean, and P. Lonergan, Solar cycle variability, ozone, and climate, *Science*, 284, 305–308, 1999.
- Svensmark, H., and E. Friis-Christensen, Variation of cosmic ray flux and global cloud coverage - a missing link in solar-climate relationships, *J. Atmos. Terr. Phys.*, 59, 1225–1232, 1997.
- Theiler, J., and D. Prichard, Constrained-realization Monte-Carlo method for hypothesis testing, *Physica D*, 94, 221–235, 1996.
- van Loon, H., and K. Labitzke, Review of the decadal oscillation in the stratosphere of the northern hemisphere, *J. Geophys. Res.*, 98, 18,919–18,922, 1993.
- van Loon, H., and D. J. Shea, The global 11-year solar signal in July–August, *Geophys. Res. Lett.*, 27, 2965–2968, 2000.
- White, W. B., J. Lean, D. R. Cayan, and M. D. Dettinger, Response of global upper ocean temperature to changing solar irradiance, *J. Geophys. Res.*, 102, 3255–3266, 1997.